

Dextran–Lipase Conjugates as Tools for Low Molecular Weight Ligand Immobilization in Microarray Development.

Sonia Herranz[†], Marzia Marciello[‡], David Olea[‡], Margarita Hernández[#], Concepción Domingo[#], Marisela Vélez^{‡,¥}, Levi A. Gheber[§], Jose M. Guisan^{‡,*}, Maria Cruz Moreno–Bondi^{†,*}

[†]Department of Analytical Chemistry, Faculty of Chemistry, Complutense University. 28040 Madrid (Spain). [‡]Department of Biocatalysis. Institute of Catalysis and Petroleochemistry–CSIC. Cantoblanco 28049 Madrid (Spain). [#] Instituto de Estructura de la Materia–CSIC . 28006 Madrid (Spain). [¥]Instituto Madrileño de Estudios Avanzados en Nanociencia, Cantoblanco 28049. Madrid (Spain). [§]Department of Biotechnology Engineering, Ben–Gurion University of the Negev, Beer–Sheva 84105 (Israel).

*** To whom correspondence should be addressed.**

E-mail: mcmbondi@quim.ucm.es; jmguisan@icp.csic.es

This file includes:

Table 1S, 2S

Figures 1S - 7S

Supporting Information

Subsection 1. Figures of merit

Table 1S. Analytical performance of microarrays prepared by patterning MCLR or MCLR-dextran-BTL2 conjugates, of various molecular weights, on planar waveguides.

	MCLR pattering	Covalent MCLR immobilization on aminated dextran–BTL2 conjugates				
		1500	6000	9000–11000	15000–25000	40000
LOD, $\mu\text{g L}^{-1}$	0.17 ± 0.05	0.11 ± 0.02	0.013 ± 0.002	0.030 ± 0.006	0.028 ± 0.006	0.025 ± 0.007
IC ₅₀ , $\mu\text{g L}^{-1}$	0.7 ± 0.1	0.48 ± 0.09	0.27 ± 0.02	0.42 ± 0.04	0.48 ± 0.07	0.25 ± 0.02
DR, $\mu\text{g L}^{-1}$	0.22 – 1.7	0.18 – 1.2	0.035 – 2.5	0.075 – 2.6	0.073 – 2.6	0.044 – 1.4

[MCLR]_{pattering} = 30 $\mu\text{g mL}^{-1}$; [anti–MC antibody] = 0.3 $\mu\text{g mL}^{-1}$; n = 3 calibration plots (\pm ts/ \sqrt{n} , 95% confidence limit)

Table 2S. Analytical performance of microarrays prepared by patterning MCLR on aminated (6000 molecular weight) dextran functionalized planar waveguides. [MCLR]_{patterning} = 30 $\mu\text{g mL}^{-1}$; [anti-MC antibody] = 0.3 $\mu\text{g mL}^{-1}$; n = 9 calibration plots.

Covalent MCLR immobilization on aminated (6000 molecular weight) dextran functionalized waveguides	
LOD, $\mu\text{g L}^{-1}$	0.10 ± 0.02
IC ₅₀ , $\mu\text{g L}^{-1}$	0.81 ± 0.04
DR, $\mu\text{g L}^{-1}$	0.24 – 2.2

(\pm ts/ \sqrt{n} , 95% confidence limit)

Subsection 2. Surface functionalization

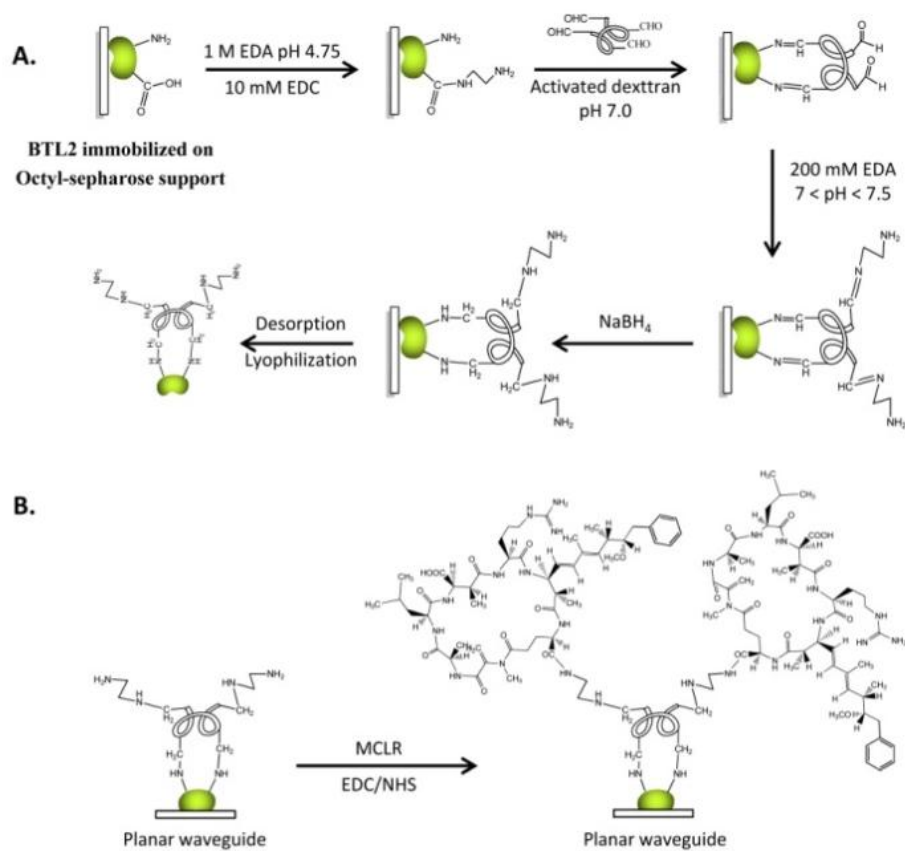


Figure 1S. (a) Scheme of the synthesis of dextran–BTL2 conjugates. (b) Waveguide functionalization with the MCLR–dextran–BTL2 conjugates.

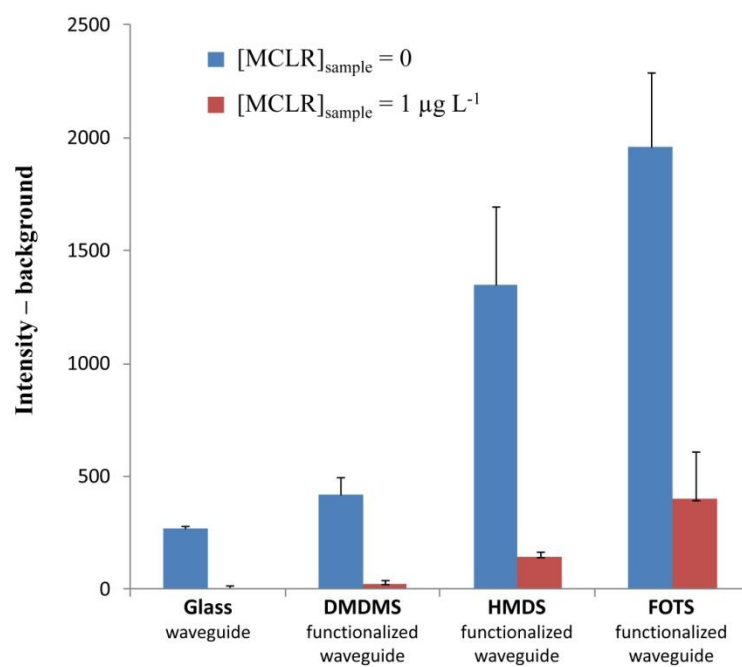


Figure 2S. Effect of silane functionalization of the planar waveguide on biosensor response. [(6000 molecular weight) dextran–BTL2 conjugate] = 0.5 mg mL⁻¹; [MCLR]_{patterning} = 30 µg mL⁻¹; [Anti–MC Ab] = 0.2 µg mL⁻¹; [Labelled–Ab] = 2.5 µg mL⁻¹; n = 3

Subsection 3. AFM Characterization

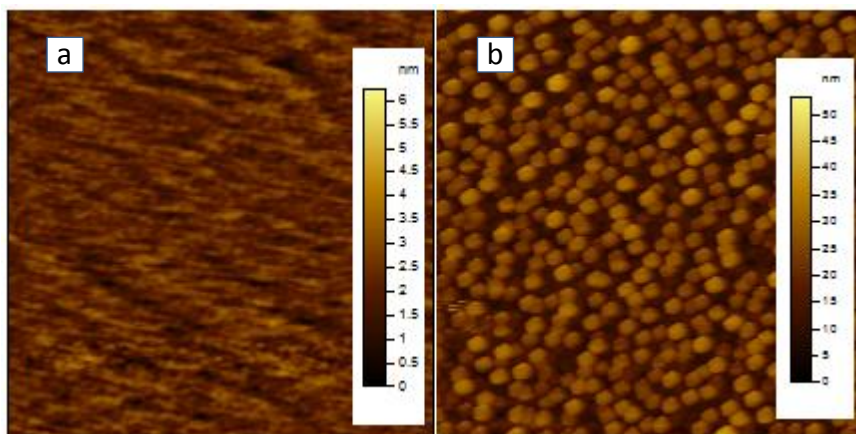


Figure 3S. AFM topography of (a) HDMS silanized glass waveguide and (b) FOTS silanized glass waveguide.

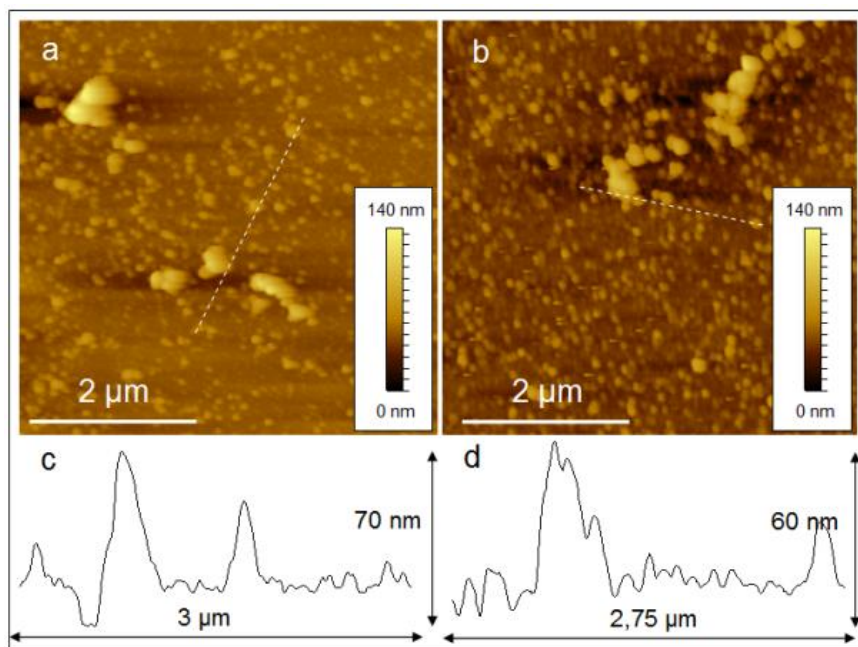


Figure 4S. AFM topography corresponding to a HMDS functionalized waveguide patterned with MCLR: (a) after incubation with anti-MC Ab, $1 \mu\text{g mL}^{-1}$ (20 min); (b) after the revealing step with the labeled Ab, $10 \mu\text{g mL}^{-1}$ (20 min). (c) and (d) show the topography profiles following the lines in (a) and (b), respectively.

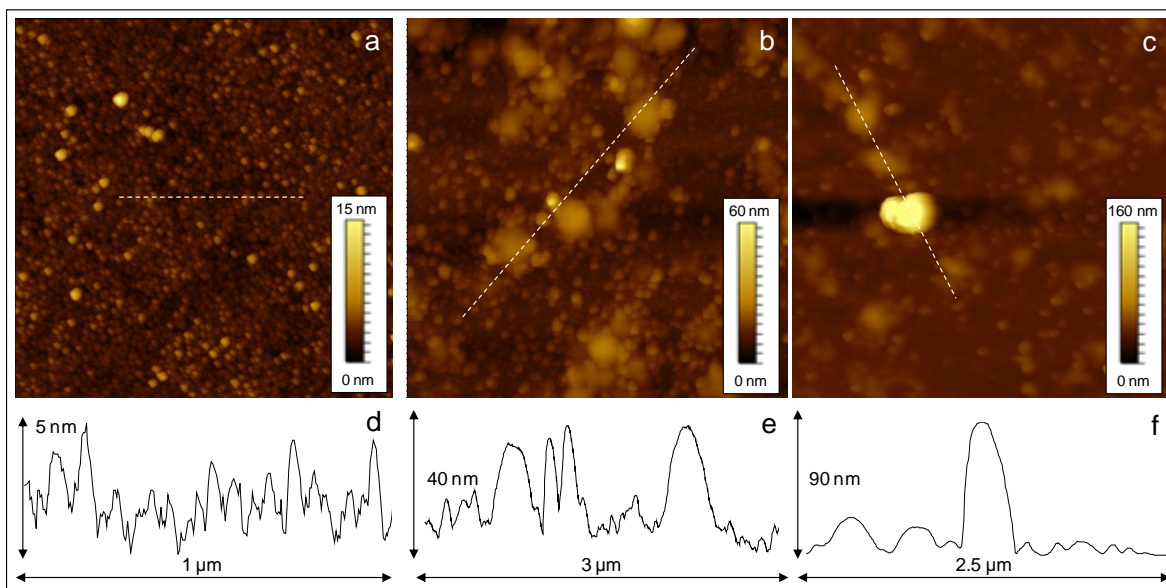


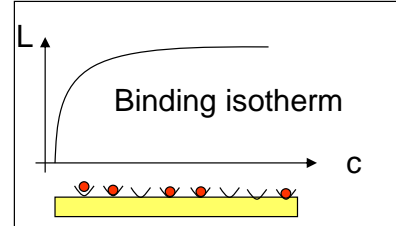
Figure 5S. (a) AFM topographic image corresponding to an aminated (6000 molecular weight) dextran functionalized waveguide. (b) AFM topographic image of the MCLR (6000 molecular weight) dextran sensor surface after incubation with anti-MC Ab ($1 \mu\text{g mL}^{-1}$, 20 min). (c) AFM topographic image of the waveguide surface after the revealing step. (d) Topographic profile following the dashed line in a. (e) Topographic profile following the dashed line in b. (f) Topographic profile following the dashed line in c.

Subsection 4. Sips equation: a discussion

Two extreme limits are known in what concerns description of binding mechanisms of a ligand to a surface (adsorption).

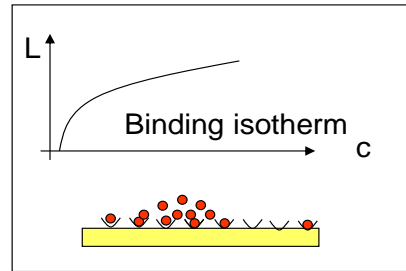
1. The Langmuir model, assuming all binding sites bind the ligand with an equal binding energy, and are able to bind one ligand each (the binding energy of a binding site vanishes once a ligand is bound). The Langmuir equation (S1) describes the formation of a monolayer, with a clear saturation behavior once all the binding sites are occupied by ligands.

$$(S1) \quad L = L_{\max} \frac{k_A C}{1 + k_A C} = L_{\max} \frac{C}{k_D + C}$$



2. The Freundlich model (S2), an empirical model describing, however, very successfully multi-layer adsorption of ligands, a so-called “piling-up” kind of adsorption. In the Freundlich limit, the adsorbed layer does not saturate, albeit it builds up at slower pace, as it grows.

$$(S2) \quad L = (kC)^\alpha$$



The Freundlich equation suffers from two drawbacks: a. it never saturates, a non-physical effect, and b. it is empirical, thus the underlying mechanism leading to this kind of behavior is unclear. These drawbacks led Robert Sips (J. Chem. Phys. **16** (5), 1948) to develop a model that is also known as the Langmuir-Freundlich equation.

3. In his seminal paper (cited above), Sips is looking for the distribution of binding energies leading to a binding isotherm such as the Freundlich (empirical) model. As a result, he formulates the Sips equation (S3):

$$(S3) \quad L = L_{\max} \frac{(kC)^\alpha}{1 + (kC)^\alpha}$$

later re-written in a more compact way as (S4):

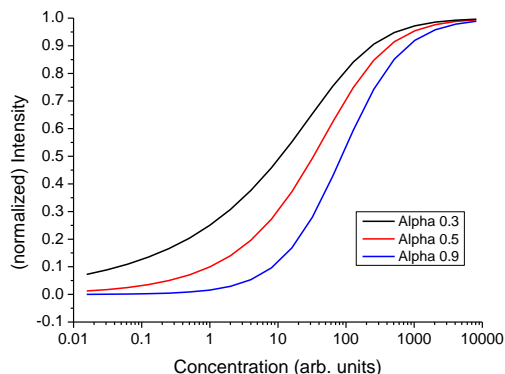
$$(S4) \quad L = L_{\max} \left(\frac{c}{k + c} \right)^\alpha$$

which is the complementary of equation (2) in the manuscript (in our case, an inhibition assay). The importance of the Sips equation is its ability to describe both extremes treated by Langmuir and Freundlich, and all the regimes in-between, as a function of a single parameter, α . As is evident from equation S3, for $\alpha=1$, the Sips equation reduces to the Langmuir equation (S1). However, for low concentrations, such that $kC \ll 1$, it reduces to

Freunlich equation (S2), with the added advantage, of course, that it saturates at high concentrations ($kC \gg 1$). The parameter α describes a distribution of binding sites that is extremely narrow (α function) for $\alpha=1$ (consistent with the Langmuir model), and increasingly broader (and resembling a Gaussian distribution) as α becomes smaller ($\alpha=0$ is non-physical, yielding a uniform distribution of binding energies).

Thus, an ν value close to 1 describes a monolayer-like binding mechanism, close to the ideal Langmuir model, while an α value significantly lower, describes a wide distribution of binding energies and results in an equation closer to the Freundlich equation, which describes and accumulation (“pile-up”) binding mechanism, as expected in a 3D fashion of stacking.

Moreover, α measures the slope of the adsorbed ligand fraction vs. free ligand fraction. In a fluorescence detection scheme, it describes the slope of fluorescence intensity vs. analyte concentration curve, as demonstrated in the adjacent figure. The lower the value of α , the more 3D the binding mechanism is, leading to a shallower slope of the “linear” portion of the curve, and thus an increased dynamic range.



This is precisely what we are observing, as we increase the molecular weight of dextran: an optimal (low) value of α for the 6000 molecular weight dextran.

This analysis rules out the possibility that we are observing simply a higher density of binding sites, however still in 2D. In terms of the equations presented above, a higher density of binding sites merely changes the value of “ L_{max} ”. A higher density of binding sites will not, however influence the parameter α . A mere increase of binding site density will not change our curves, because they are normalized between 0 to 1. The change in their slope (α), though, clearly indicates an increasing binding in 3D, in the volume of the layer.

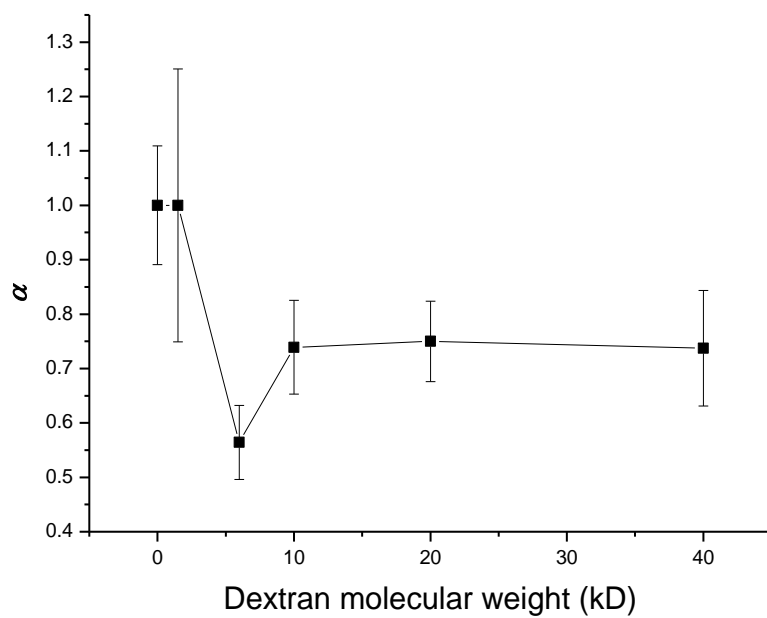


Figure 6S. The Sips parameter α as a function of dextran molecular weight. $\alpha = 1$ indicates monolayer (Langmuir-like) binding, while smaller α values indicate progressively 3D binding.

Subsection 6. Biosensor long term stability

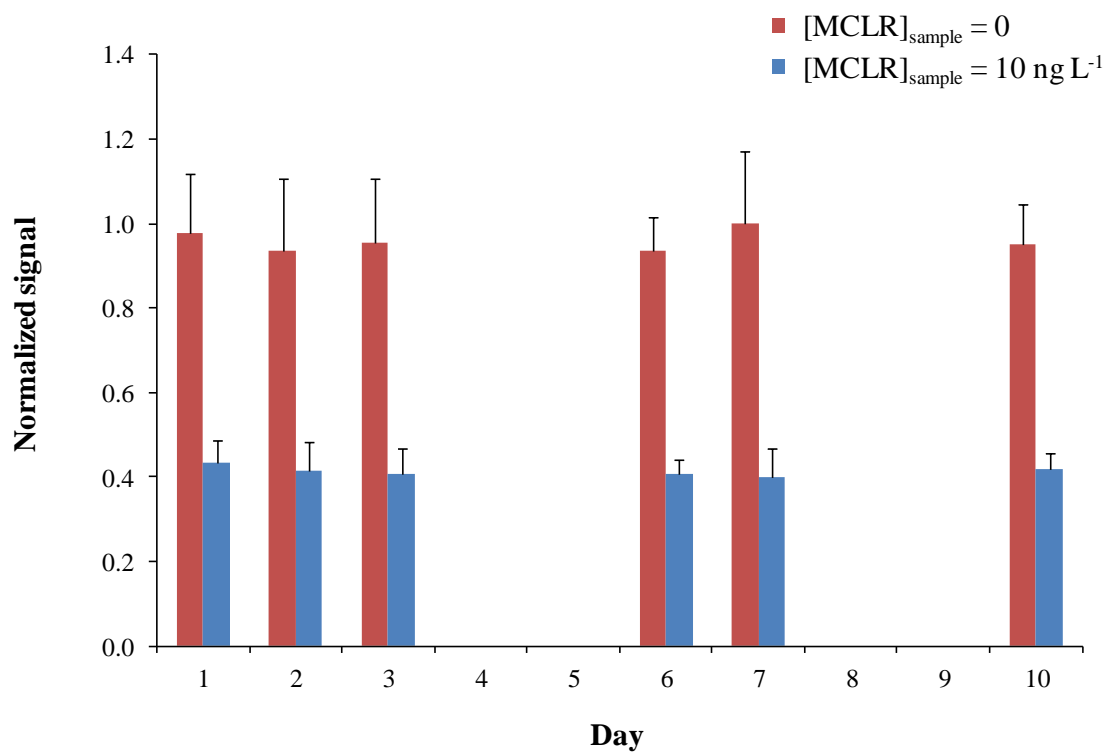


Figure 7S. Biosensor response, in the optimum conditions, in the absence and in the presence on 10 ng L^{-1} MCLR over a period of 10 days after waveguide preparation ($n = 9$).